

## 3.9 ECM DECEPTION OFF-BOARD

Deceptive off-board electronic countermeasures are countermeasures deployed from the target aircraft and designed to generate false targets or to induce tracking errors by actively transmitting deceptive waveforms. ESAMS version 2.7 provides the capability to model effects of two types of off-board ECM, chaff and towed decoys. The effectiveness of chaff and towed decoys is an important aspect of many aircraft survivability analyses, and its prediction is an important design objective of ESAMS. This section will examine some of the modeling characteristics and sensitivities of chaff and towed decoys as modeled in ESAMS.

### 3.9.1 Chaff

Chaff is probably the oldest and most widely used type of deceptive ECM. Chaff typically consists of a large number of dipole reflectors, usually in the form of aluminum filaments or aluminized-glass, which are packaged as a bundle. The dipoles are cut with different lengths so that they resonate over a range of frequencies that cover the threat radars of interest. While the individual chaff bundles are physically small, when release from the aircraft, the chaff filaments scatter or 'bloom' and the RCS increases in proportion to the physical size of the chaff cloud. Chaff clouds present false targets to the ground-based tracking radar or missile seeker, and if effective, can decoy the missile away from the aircraft.

ESAMS models chaff clouds deployed in the aircraft wake. Chaff clouds are the most common type of chaff but because they are deployed behind the aircraft and decelerate rapidly, they can often be distinguished from the intended target by human operators or by automated techniques, such as, e.g., leading-edge trackers. Forward-fired chaff rockets, which are not modeled in ESAMS, will generate false targets in front of the target and may be more effective against radars with counter-countermeasures designed for cloud chaff.

#### 3.9.1.1 Objectives and Procedures

The objective of this analysis is to examine some of the chaff characteristics including frequency response, cloud bloom rate, chaff speed and effective RCS as modeled in ESAMS and to compare chaff effectiveness for targets of different RCS.

#### 3.9.1.2 Frequency Response

The chaff frequency response is computed in subroutine CLDRCS. The inputs to this subroutine are the number of dipole types, the number of dipoles of each type, and their length. In normal model execution, the radar wavelength is passed in and the chaff response is computed. To obtain the chaff response over a range of wavelengths (or frequencies), a simple driver was developed that called CLDRCS for the range of interest.

#### 3.9.1.3 Cloud Bloom Rate

To obtain the chaff cloud size as a function of time from deployment, a write statement was added in subroutine CHFRCS to print the value of the presented area (variable AREAP). Since the ESAMS algorithm expands the cloud slightly faster in the direction parallel to the target velocity than perpendicular to it, the projected cloud area will be somewhat dependent on the viewing aspect. For this analysis, a crossing target profile was selected so the viewing angle was approximately perpendicular to the cloud.

### **3.9.1.4 Chaff Speed**

Chaff speed is an important characteristic that can permit chaff discrimination from the intended target. Chaff decelerates rapidly once deployed and may be effectively countered by MTI or Doppler processing or by special tracking techniques such as leading-edge tracking. The chaff speed is computed in subroutine CHFCLD using a constant deceleration. The appropriate equation was used to independently generate plots of chaff speed as a function of different initial target velocities.

### **3.9.1.5 Effective Chaff RCS**

The effective chaff RCS is also computed in subroutine CHFRCS and was printed out for the same target profile used to obtain the cloud projected area.

### **3.9.1.6 Chaff Effectiveness**

Chaff effectiveness was determined by whether the chaff was successful in achieving a radar break-lock or not. Various straight and level target profiles were run with different target signatures. The missile flyout was disabled, the acquisition time was set to zero, and one chaff round was deployed. A sample input listing is presented in Figure 3.9-1. The magnitude of target tracking errors in azimuth and elevation were examined to determine when a break-lock occurred.

```

RUNID      1
SXT        2500 5000 1000
SVT        250          (vel 250 m/s)
SPSIT      180          (aircraft heading)
ACQTIM     0
TRKTIM     20
FDEL       20
EXEFLY     0          (no missile flyout)
RDECMD     1          (read ecmd data file)
DVECMD     19         (ecmd logical unit)
CDECMD     8          (read chaff data)
          END

ECMD
PARC       1
TCHAFF     5          (one burst at 5 sec)
DTCHF      15.
DPDEL      15.
          END

TGTS
PTRSIG     1
SIGTBL     2  2
           0    180
           0  0.1  0.1  (0.1 sq m target RCS)
           180 0.1  0.1
          END

END RUN

```

FIGURE 3.9-1. Sample ESAMS Input file for Chaff Run.

## 3.9.2 Results

### 3.9.2.1 Frequency Response

The default chaff characteristics modeled in ESAMS are not identified in the ESAMS documentation as any specific chaff type but contain nine dipole types of different length and numbers. ESAMS approximates the response of the cloud by using five discrete scatterers whose individual RCS is a function of frequency. The frequency response for the default chaff type is plotted in Figure 3.9-2.

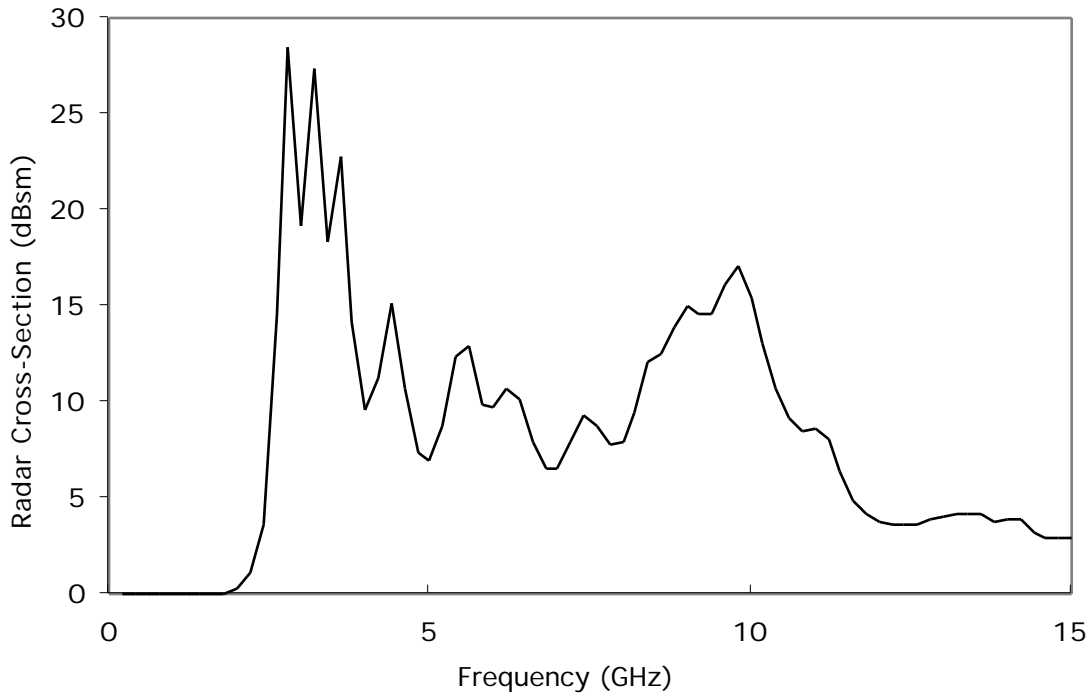


FIGURE 3.9-2. Chaff-Generated Radar Cross-Section per Scatterer.

### 3.9.2.2 Cloud Bloom Rate

Unlike the chaff modeling in previous versions of ESAMS which assumed that the chaff cloud bloomed instantaneously, version 2.7 uses a more realistic assumption that disperses the cloud as a function of time. This is done by randomly computing the scatterer positions from a normal distribution with time-dependent dispersions given by:

$$\sigma_{\perp}(t) = \frac{v_R}{\sqrt{2}} \left[ 1 - \exp(-t / \tau_{\perp}) \right] \quad [3.9-1]$$

$$\sigma_{\parallel}(t) = \tau_{\parallel} \left[ 1 - \exp(-t / \tau_{\parallel}) \right]$$

where  $\sigma_{\perp}$  and  $\sigma_{\parallel}$  are the dispersions perpendicular and parallel to the target velocity.

The default values for the various constants in Eqs. 3.9-1 yield a projected cloud area that grows as a function of time as illustrated in Figure 3.9-3. The fluctuations are caused by the random positions of the individual scatterers at each evaluation step.

Theoretical and empirical analysis has established that the RCS of a chaff cloud can be approximated by the expression:

$$RCS = A_o \left[ 1 - \exp(-n_k) \right] \quad [3.9-2]$$

where  $n_k$  is the number of dipoles of type,  $k$ , per unit of cloud projected area. When the number of dipoles is large, the RCS of the cloud is approximately equal to the projected cloud size:  $\sigma = A_0$ .

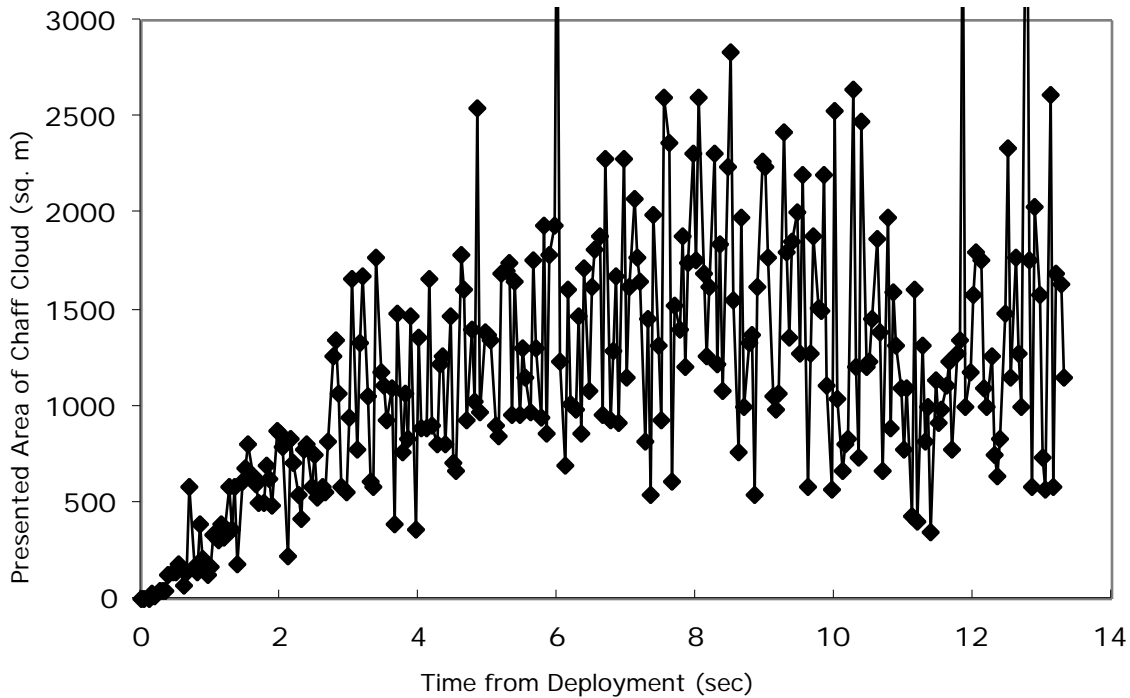


FIGURE 3.9-3. Presented Area of Chaff Cloud as a Function of Time From Deployment.

### 3.9.2.3 Chaff Speed

The chaff speed is computed with a constant deceleration in subroutine CHFCLD using the equation:

$$v(t) = v(0) - 914.4 t \quad [3.9-3]$$

where  $v(0)$  is the target velocity at the time of chaff deployment.

Plots of chaff speed for several initial target velocities are illustrated in Figure 3.9-4 and show that the mean chaff velocity decays to zero in less than a third of a second for target velocities up to 300 m/s.

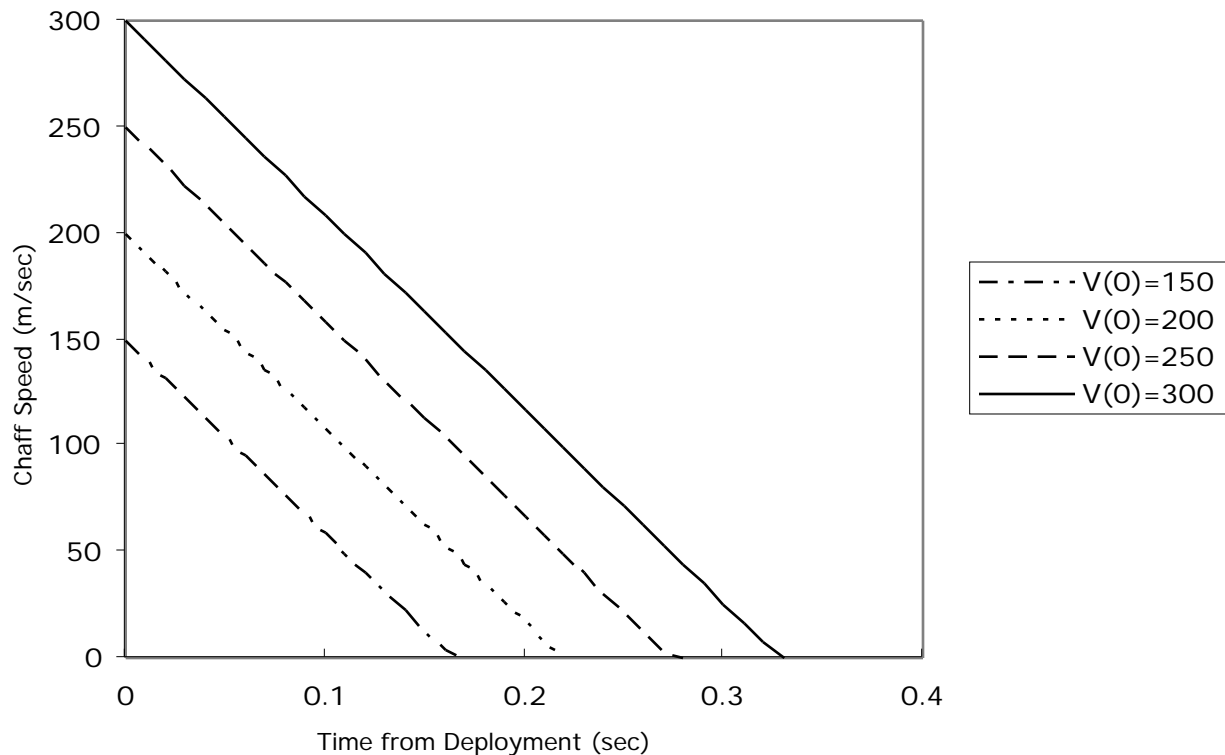


FIGURE 3.9-4. Chaff Speed as a Function of Time From Deployment.

### 3.9.2.4 Effective Chaff RCS

As mentioned earlier, independent research has shown that the effective chaff RCS is approximately equal to the projected cloud area when the number of chaff dipoles divided by the area is large. ESAMS goes to some length to model the chaff cloud and compute its projected area as a function of time, but in subroutine CHDPLR, the maximum effective chaff RCS is limited to the RCS of a single scatterer. This limiting value is frequency dependent, and for the frequency used in these sensitivity analyses (14.8 GHz) was  $2.9 \text{ m}^2$  (see Figure 3.9-2 above).

### 3.9.2.5 Chaff Effectiveness

The way the ESAMS tracking algorithm is implemented, chaff will be effective in pulling the track radar or missile seeker off the target whenever the chaff power return is greater than the target power. With no MTI or Doppler processing, this condition is satisfied whenever the chaff RCS is greater than the target RCS. With MTI or Doppler processing, it is possible that the chaff signal could be attenuated below the target return before achieving break-lock.

Azimuth tracking errors as a function of time are plotted in Figure 3.9-5 for target signatures of 10, 1.0, and  $0.1 \text{ m}^2$ . The target profile starts at 2500m uprange with a 5000m offset, and the target velocity is 250 m/s. One chaff bundle is released at 5sec when the target is perpendicular to the radar site. For target signatures of  $3 \text{ m}^2$  and larger, chaff is

ineffective. For smaller target signatures, chaff is effective. MTI did not affect the chaff effectiveness for the engagement geometries examined.

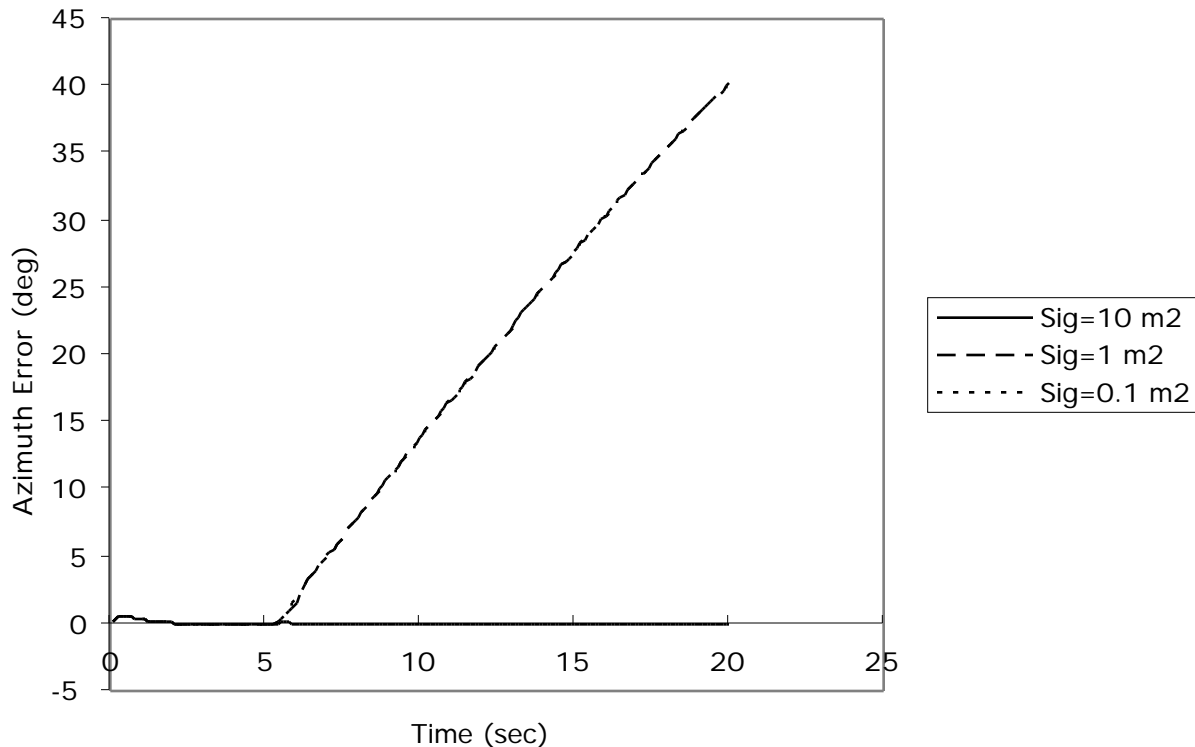


FIGURE 3.9-5. Azimuth Tracking Errors as a Function of Time.

### 3.9.2.6 Conclusions

The chaff frequency response, cloud bloom rate, and chaff speed characteristics all seem to be reasonable. The chaff RCS grows initially as the size of the presented chaff cloud area, but once the cloud area exceeds the dipole response, the chaff RCS is reset to the (smaller) dipole RCS. This has the effect of arbitrarily limiting the chaff effectiveness to target signatures of approximately the same or smaller RCS. An MDR has been submitted to the ESAMS CCB to remove this restriction in subroutine CHFRCS.

### 3.9.3 Towed Decoy

Another type of (expendable) off-board countermeasure is the towed decoy. Unlike chaff which is always passive and only reflects radar energy, a towed decoy may be passive or active. An active decoy is one that transmits radar energy usually at the frequency of the threat radar and may simply repeat the received waveform with amplification or may superimpose deception techniques such as range and/or velocity gate pull off. The effectiveness of the towed decoy will depend on a number of parameters including tow length, jammer power, antenna gain, and the nature of any deceptive waveforms generated.

### 3.9.3.1 Objectives and Procedures

The objective of this analysis is to examine the effectiveness of a towed decoy using only repeater techniques, i.e. no deception jamming is considered. The parameters to be varied are tow length and jammer power which is input as the relative jammer-to-signal (J/S) ratio. These were varied through an overlay to the default ECMD data file. The passive RCS of the decoy used was the default value of  $1.0 \text{ m}^2$  and a target RCS of  $10 \text{ m}^2$  was input. A sample input listing is presented in Figure 3.9-6.

```

RUNID      1
SXT        0  4000  1000
SVT        250          (vel 250 m/s)
SPSIT      180          (aircraft heading)
RNOISE     1
INOISE     1  1  1  1
PRFTBL     <2> 0.1
RDECMD     1          (read ecmd data file)
DVECMD     19         (ecmd logical unit)
CDECMD     9          (read towed decoy data)
          END
ECMD
DISMAX     50          (tow length)
ECMT       <1>  2  2  (ANTENNA PATTERN 2D TABLE)
          0.0  180.0
          0.0  0.0  0.0
          180.0 0.0  0.0
ECMT       <200>  2  (ECM POWER)
          0.0  10.0  8.0  10.0
ECMT       <600>  2  (ECM TIME DELAY)
          0.0  0.00000  8.0  0.00000
          END
END RUN

```

FIGURE 3.9-6. Sample ESAMS Input File for Towed Decoy Run.

### 3.9.3.2 Results

Like chaff effectiveness, the towed decoy effectiveness is also geometry-dependent. The decoy power and tow length variations were done with a single crossing target profile having an offset of 4000m and the miss distances as a function of J/S are presented in Figure 3.9-7. A more continuous transition in miss distances from zero to the tow length was expected. The ESAMS results indicate that the threat radar either tracks the target or tracks the decoy and that there is very little target-decoy centroiding or phase interference.



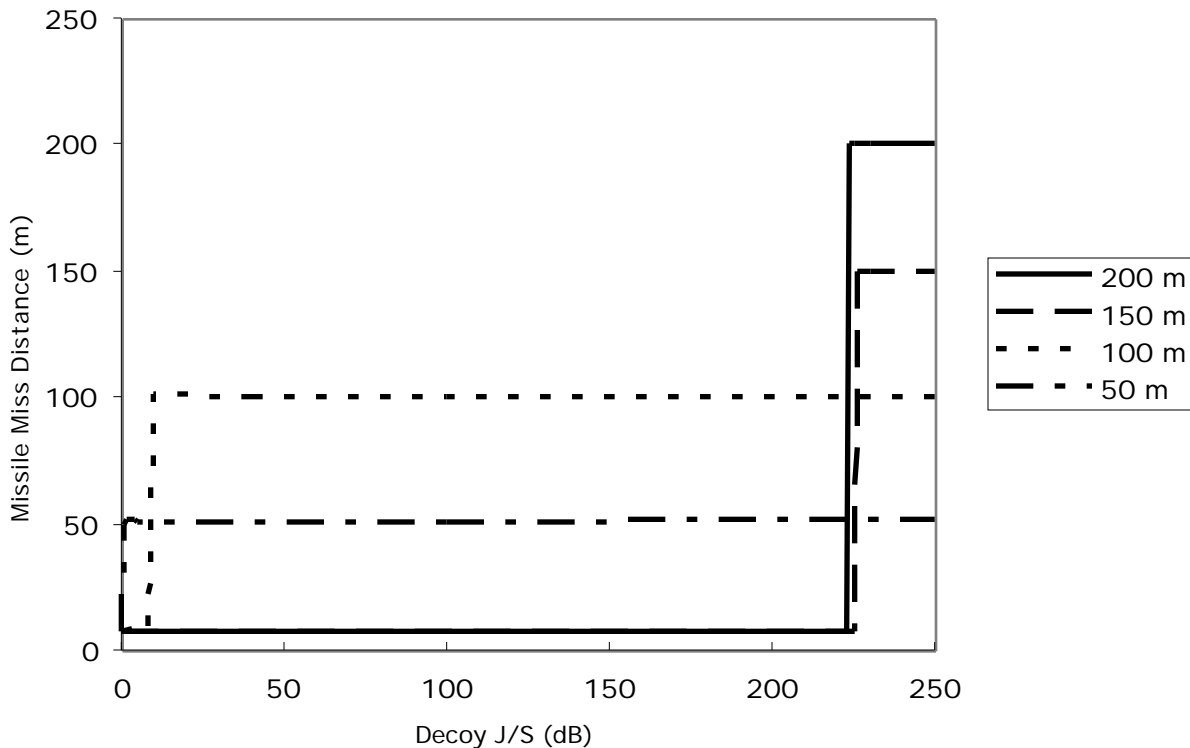


FIGURE 3.9-7. Missile Miss Distance as a Function of Towed Decoy J/S for Various Tow Lengths.

The second interesting feature of these results is the relatively large increase in power required to decoy the missile when going from the 100 m to 150 m tow length. Detailed analysis showed that these results are a consequence of using several of the default ECMD parameters for deploying and activating the towed decoy. Decoy deployment is specified by the variable, DCYTIM, which is defaulted to 3 sec in the ECMD file. The time at which the decoy transmitter is activated is determined by TIMEON and the mode type, TECMOD, with can specify acquisition, track, seeker modes or time-to-go, etc. The defaults are TIMEON=3 sec and TECMOD=3 (track mode); therefore, the decoy repeater waveform will be activated after 3 seconds of target tracking. With the default two-second acquisition time and 2-second track establishment time, this means that the decoy is deployed one second prior to missile launch and the jamming signal is activated 1 second after missile launch.

This explains why the power requirements for decoy effectiveness are so much higher for the 150 and 200 m tow lengths. When the decoy jamming is activated for the 150 m and 200 m tow lengths, the decoy is no longer in the mainbeam of the tracking antenna, and consequently, the power required is higher. This can be confirmed by examining the antenna gain for the threat system used which is plotted in Figure 3.9-8. The target-decoy azimuth separation at 10 seconds after missile launch is also plotted for each tow length, and one can see that for the 150 and 200 m tow lengths, the decoy is out of the antenna mainbeam. Figure 3.9-8 also explains why slightly more power is required by the decoy

with a 150 m tow length than at 200 m: at 150 m the decoy is close to an antenna null while at 200 m, it is in the first sidelobe.

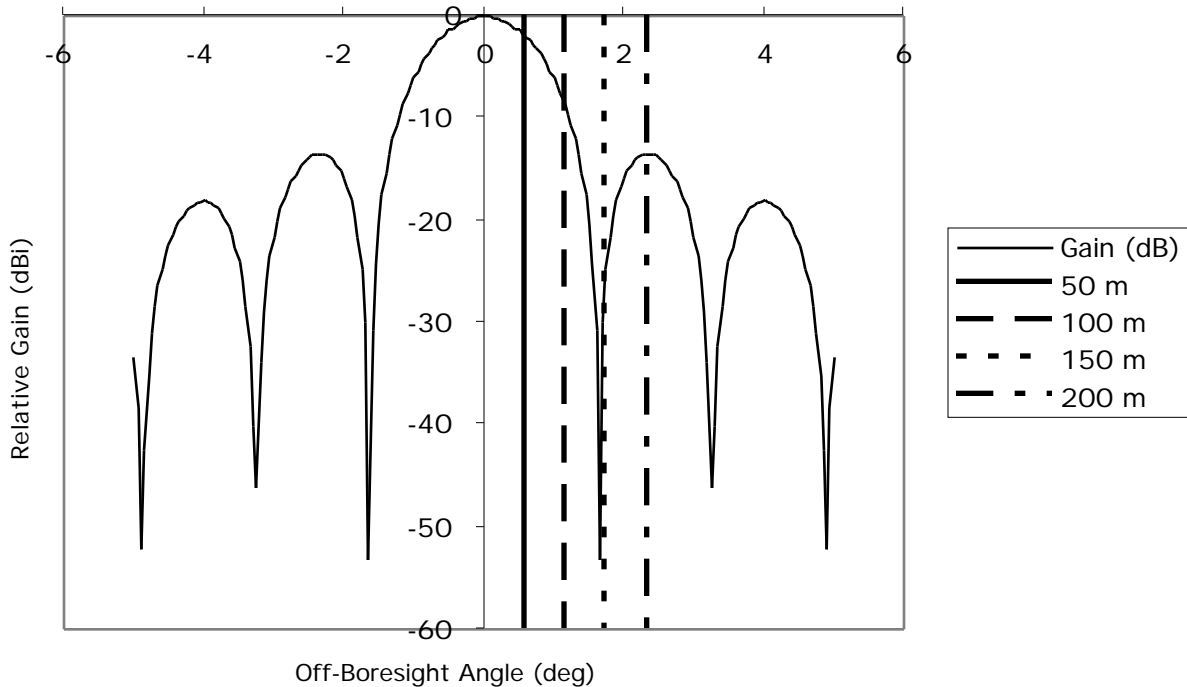


FIGURE 3.9-8. Antenna Azimuth Beamshape with Target-decoy Angular Separation for the Tow Lengths Used.

One would expect that if the decoy J/S were sufficient, the radar would track the decoy from the time it separated from the aircraft until it reached its maximum tow length. In order to test this, the J/S and tow length sensitivities were rerun with three changes:

|              |                     |
|--------------|---------------------|
| ACQTIM=0     | (PROGC)             |
| TIMEON=0.001 | (ECMD)              |
| DCYTIM=0.001 | (ECMD) <sup>1</sup> |

Miss distance as a function of J/S with the decoy activated immediately is plotted in Figure 3.9-9. With tow lengths of 50 and 100 m, the decoy is effective at J/S ratios less than one. This is not unreasonable since the engagement involves a receding target. The ground-based tracking radar initially tracks the target then switches to the decoy in the course of the engagement.

<sup>1</sup>. DCYTIM was set to 0.001 because if it is zero identical to zero, the decoy will never be deployed. The check for decoy deployment in subroutine TDDPLY (line 62) uses DCYTIM greater than zero (rather than greater than or equal to zero).

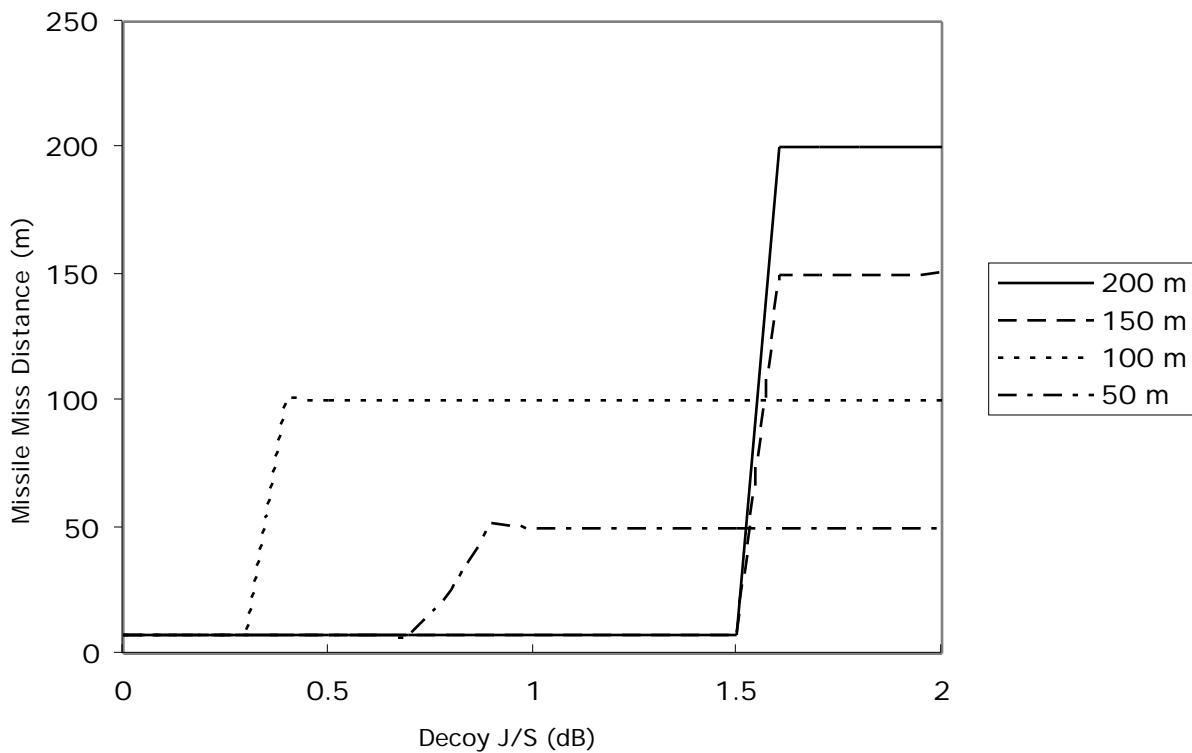


FIGURE 3.9-9. Missile Miss Distance as a Function of Towed Decoy J/S for Various Tow Lengths. Decoy is Activated Immediately.

### 3.9.3.3 Conclusions

Towed decoys are usually employed as self-protection ECM against semi-active missiles. The towed decoy option in these sensitivity analyses was exercised against the ground-based target tracking radar for a command-guided SAM, but the results are expected to be similar for semi-active missiles. This analysis was also restricted to repeater-type jamming and did not examine the effectiveness of deceptive jamming, e.g. RGPO, VGPO, etc., by the decoy. The results show a significant sensitivity to jammer J/S, tow length, and time of activation; however, all the trends seem reasonable based on a detailed examination of the modeling assumptions (e.g., no glint, scintillation, etc.).

